

Fast Video Object Segmentation using the Global Context Module

Yu Li^{1*} Zhuoran Shen^{2*†} Ying Shan¹

¹Tencent PCG Applied Research Center ²The University of Hong Kong
 {ianyili, yingsshan}@tencent.com shenzhuoran@connect.hku.hk

Abstract

We developed a real-time, high-quality video object segmentation algorithm for semi-supervised video segmentation. Its performance is on par with the most accurate, time-consuming online-learning model, while its speed is similar to the fastest template-matching method which has sub-optimal accuracy. The core in achieving this is a novel global context module that reliably summarizes and propagates information through the entire video. Compared to previous approaches that only use the first, the last, or a select few frames to guide the segmentation of the current frame, the global context module allows us to use all past frames to guide the processing. Unlike the state-of-the-art space-time memory network that caches a memory at each spatiotemporal position, our global context module is a fixed-size representation that does not use more memory as more frames are processed. It is straightforward in implementation and has lower memory and computational costs than the space-time memory module. Equipped with the global context module, our method achieved top accuracy on DAVIS 2016 and near-state-of-the-art results on DAVIS 2017 at a real-time speed.

1. Introduction

Video object segmentation aims to segment a foreground object from the background for all frames in a video. The task has numerous applications in computer vision. An important application is intelligent video editing. As video becomes the most popular form of media on mass content platforms, video content creation is getting increasing levels of attention. Object segmentation on each frame with image segmentation tools is time-consuming and has poor temporal consistency. Semi-supervised video object segmentation tries to solve the problem by segmenting the object in the whole video guided only by a fine object mask on the first frame. This problem is challenging since object

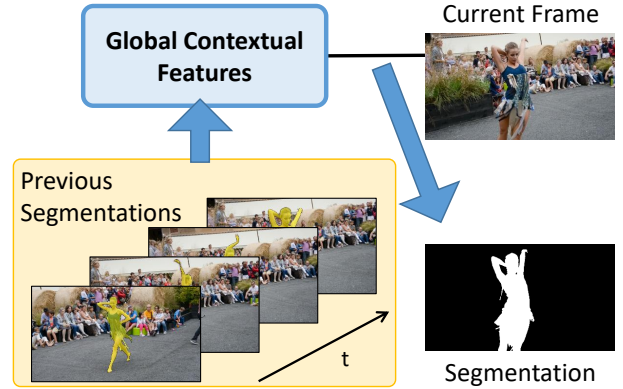


Figure 1. Our video object segmentation method predicts the object mask at the current frame in the video by maintaining fixed-size global context features generated from previous frames and masks. It is efficient in both memory and computation and achieves high segmentation accuracy. See more details below.

appearance might vary drastically over time in a video due to pose changes, motion, and occlusions, etc.

With the success in many computer vision tasks, deep learning techniques are widely used in video object segmentation now. The essence is to learn an invariant representation that accounts for the variation of object appearance across frames. Some early works [2, 21, 23, 28] in semi-supervised video object segmentation use the first frame to train a model using various data augmentation strategies, which are commonly referred to as online-learning methods. These methods usually obtain accurate segmentation that are robust to occlusions. However online learning incurs huge computational costs that lead to several seconds of processing per frame. Another direction is propagation-based methods [4], which rely on the segmentation of the previous frame to infer for the current frame. These methods are simple and fast, but usually have sub-optimal segmentation accuracies. These methods cannot handle occlusions and may suffer from error drifts. Some later works take the advantages of both directions, use both the first and the previous frame [27, 30, 31, 34], and achieved both high accuracy and fast processing speed.

*Equal contributions.

†This work was done during an internship at Tencent PCG Applied Research Center

A recent work [22] made a further step to use all previous frames with the corresponding object segmentation results to infer the object mask on the current frame. It proposes a novel space-time memory (STM) module that stores the segmentation information at each processed frame, *i.e.*, this memory module saves information in all the spatiotemporal locations in previous frames. When working on a new frame, a read operation is used to retrieve relevant information from the memory by performing a dense feature correlation operation in both temporal and spatial dimensions. By using this memory that saves all guidance information, the method is robust against drastic object appearance changes and occlusions. It produces promising results and achieved state-of-the-art performance on multiple benchmark datasets.

While STM achieves state-of-the-art performance by making full use of the information from previous frames, we found leveraging the space-time memory is costly, especially on long video sequences. As STM keeps creating new memories to save new information and put it together with old memories, the computational cost and memory usage in the feature correlation step increases linearly with the number of frames. This makes the method slower and slower while processing and may cause GPU memory overflow. To resolve this issue, the authors proposed to reduce the memory saving frequency, *e.g.* saving a new memory every 5 frames. However the linear complexity with time still exists, and such reduction in memorization frequency defeats the original purpose to utilize information from every previous frame.

In this paper, building upon the idea of STM to use information in all past frames, we develop a global representation that summarizes the object segmentation information and guide the segmentation in the next frame. This representation automatically updates when the system moves forward by a frame. The core component of it is a novel global context (GC) module (illustrated in Fig. 1). By keeping only a fixed-size set of features, our memory and computational complexities for inference is constant with time, in comparison to the linear complexities of the STM module. We show that using this highly efficient global context module, our method is about three times faster than STM running on the DAVIS 2016 dataset and is the only one that has both state-of-the-art accuracy and real-time processing speed.

The contribution of our paper can be summarized as:

- We propose a novel global context module that reliably maintains segmentation information of the entire video to guide the segmentation of incoming frames.
- We implement the global context module in a lightweight way that is efficient in both memory usage and computational cost.
- Experiments on the DAVIS 2016 and 2017 datasets

show that our proposed GC module can achieve top accuracy in video object segmentation and is highly efficient that runs in real time.

2. Related works

Online-learning methods. Online-learning methods usually fine-tune a general object segmentation network on the object mask of the start frame to teach the network to identify the appearance of the target object in the remaining video frames [2]. They use online adaptation [28], instance segmentation information [21], data augmentation techniques [15], or an integration of multiple techniques [20]. Some methods reported that online learning boost the performance of their model [18, 30]. While online learning can achieve high-quality segmentation and is robust against occlusions, it is computationally expensive as it requires fine-tuning for each video. This huge computational burden makes it impractical for most applications.

Offline-learning methods. Offline-learning methods use strategies like mask propagation, feature matching, tracking, or a hybrid strategy. Propagation-based methods rely on the segmentation mask of the previous frame. It usually takes the previous mask as an input and learns a network to refine the mask to align it with the object in current frame. A representative work is MaskTrack [23]. This strategy of using the previous frame is also used in [1, 35]. Many works [5, 13, 23] also use optical flow [7, 12] in the propagation process. Matching-based methods [3, 11, 26, 27, 30, 31] treat the first frame (or intermediate frames) as a template and match the pixel-level feature embeddings in the new frame with the templates. A more common setup is to use both the first and the previous frames [27, 30, 31], which cover both long-term and short-term object appearance information.

Space-time memory network. The STM network [22] is a special feature matching-based method which performs dense feature matching across the entire spatio-temporal volume of the video. This is achieved by a novel space-time memory mechanism that stores the features at each spatio-temporal location. The space-time memory module mainly contains two components and two operations. The two components are a key map and a value map where the key encodes the visual semantic embeddings for robust matching against appearance variations, and the value stores detailed features for guiding the segmentation. The memory write operation simply concatenates the key and value maps generated on past frames and their object segmentation masks. When processing a new frame, the memory read operation uses the key to match and find the relevant locations in the spatio-temporal volume in the video. Then the features stored in the value maps at those locations are retrieved to predict the current object mask.

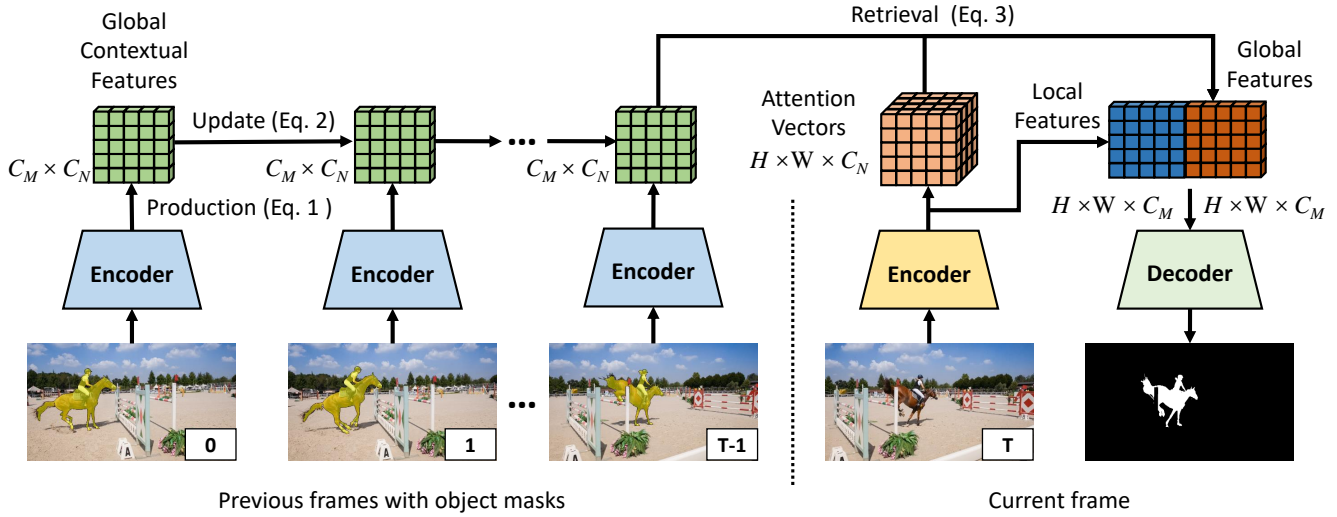


Figure 2. This is an overview of our pipeline. Our network encodes past frames and their masks to a fixed-size set of global context features. These vectors are updated by a simple rule when the system moves to the next frame. At the current frame, a set of attention vectors are generated from the encoder to retrieve relevant information in the global context to form the global features. Local features are also generated from the encoder output. The global and local features are then concatenated and passed to a decoder to produce the segmentation result for this frame. Note that there are two types of encoders, the blue one for past frames and masks (four input channels), and the orange one for the current frame (three input channels).

3. Our Method

3.1. Global Context Module

The space-time memory network [22] achieved great success in video object segmentation with the space-time memory (STM) module. The STM module is an effective module that queries features from a spatio-temporal feature store formed from previous frames to guide the processing of the current frame. This way, the current frame is able to use the features from semantically related regions in past frames to help refine its features. However, the STM module has a drawback in efficiency that it stores a pair of key and value vectors for each location of each frame in the memory. These feature vectors are simply concatenated over time when the system moves forward and their sizes keep increasing. This means its resource usage is highly sensitive to the spatial resolution and temporal span of the memory. Consequently, the module is limited to have memories with low spatial resolutions, short temporal spans, or reduced memory saving frequency in practice. To remedy this drawback, we propose the global context (GC) module. Unlike the STM module, the GC module keeps only a small set of fixed-size global context features yet retains exactly the same representational power compared to the STM module. To simplify the expressions, we assume the output to have $N = H \times W$ locations and C channels in the following sections. Fig. 2 shows the overall pipeline of our pro-

posed method using the global context module. The main structure is an encoder-decoder and the global context module is built on top of the encoder output, similarly to [22]. There are mainly two operations in our pipeline, namely 1) context extraction and update on a processes frame and its object mask, and 2) context distribution to the current frame under processing. There are two types of encoders used. One takes a color image and an object mask (ground truth mask for the start frame and segmentation results for intermediate frames) to encode the frame and segmentation information into the feature space. Another encoder encodes the current frame to a feature embedding. We distribute the global context features stored in the GC module and combine the distributed context features with local features. Then a decoder is used to produce the final object segmentation mask on this frame.

3.1.1 Context Extraction and Update

When extracting the global context features, the GC module first generates the keys and the values, following the same procedure as in the STM module. The keys and the values have size $H \times W \times C_N$ and $H \times W \times C_M$ respectively, where C_N and C_M are the numbers of channels used. Unlike the STM module that directly stores the keys and values, the GC module puts the keys and the values through a further step called global summarization.

The global summarization step treats the keys not as

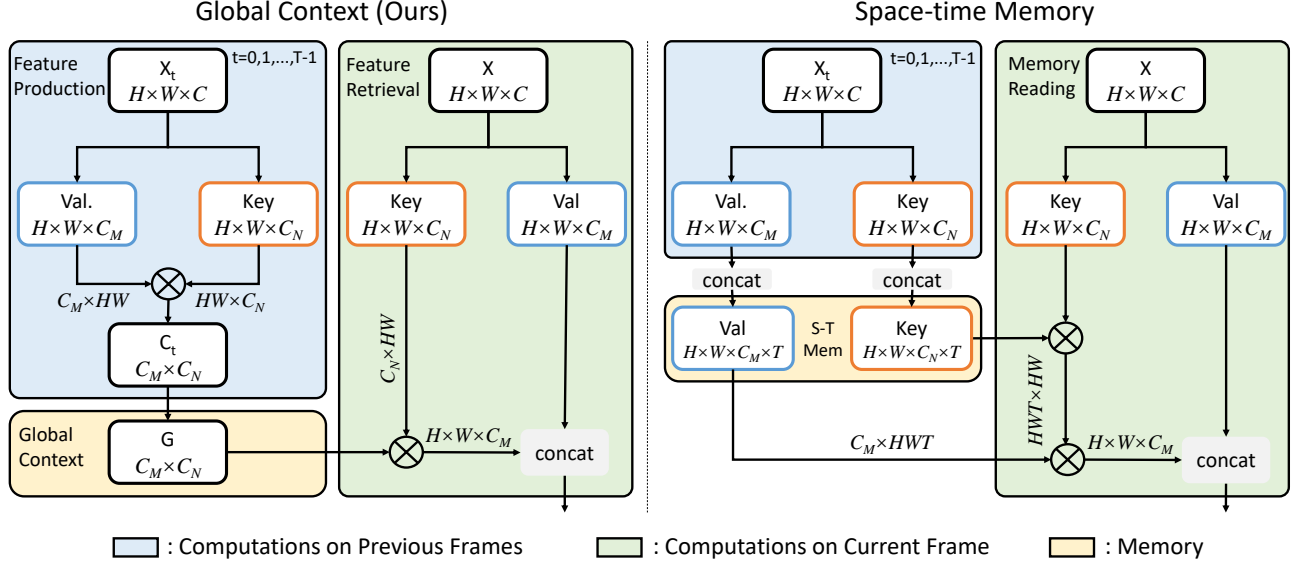


Figure 3. The detailed implementation of the GC module with a comparison to the STM module in [22].

$H \times W$ vectors of size C_M each for a location, but as C_M 1-channel feature maps each as an unnormalized weighting over all locations. For each such weighting, the GC module computes a weighted sum of the values where each value is weighted by the scalar at the corresponding location in the weighting. Each such weighted sum is called a global context vector. The GC module organizes all C_M global context vectors into a global context matrix as the output of global summarization. This step can be efficiently implemented as a matrix product between the transpose of the key matrix and the value matrix. Following is an equation describing the context extraction process of the GC module:

$$C_t = k(X_t)^T v(X_t), \quad (1)$$

where t is the index of the current frame, C_t is the global context matrix, X_t is the input to the module (output of the encoder), and k, v are the functions that generate the keys and values. Having obtained C_t , the rule for updating the global context feature is simply

$$G_t = \frac{t-1}{t} G_{t-1} + \frac{1}{t} C_t, \quad (2)$$

where G_t is the global context for the first t frames with G_0 being a zero matrix. The weight coefficients before the sum make that each C_p for $1 \leq p \leq t$ contributes equally to G_t .

3.1.2 Context Distribution

At the current frame, our pipeline distributes relevant information stored in the global context module to each pixel. In the distribution process, the GC module first produces

the query keys in the same way as the STM module. However, the GC module uses the queries differently. At each location, it interprets the query key as a set of weights over the global context features in the memory and computes the weighted sum of the features as the distributed context information. In contrast, the memory reading process of the STM module is much more complex. The STM module uses the query to compute a similarity score with the key at each location of each frame in the memory. After that, the module computes the weighted sum of the values in the memory weighted by these similarity scores. Following is an formula that expresses this context distribution process:

$$R_t = q(X)_t G_t, \quad (3)$$

where R_t is the distributed context features for frame t and q is the function generating the queries.

Surprisingly, the simple context distribution process of the GC module and the much more complex process of the STM module accomplish the same goal, which is to summarize semantic regions across all past frames that are of interest to the querying location in the current frame. The STM module achieves this by first identifying such regions via query-key matching and then summarizing their values through a weighted sum. The GC module achieves the same much more efficiently since the global context vectors of the GC module are already global summarizations of regions with similar semantics across all past frames. Therefore, the querying location only needs to determine on an appropriate weighting over the global context vectors to produce a vector that summarizes all the regions of interest to itself. For example, if a pixel is interested in persons, it could

place large weights on global context vectors that summarize faces and bodies. Another pixel might be interested in the foreground and could put large weights on vectors that summarize various foreground object categories. We will provide a mathematical proof that the GC and STM modules have exactly the same modeling power.

3.1.3 Comparison with the Space-Time Memory Module

We have plotted the detailed implementation of our global context module in Fig. 3 and compare with the space-time memory module used in [22]. There are a few places our GC has advantages in efficacy over STM.

The global summarization process is the first way the GC module gains efficiency advantage over the STM module. The global context matrix has size $C_M \times C_N$, which tends to be much smaller than the $H \times W \times C_N$ key and $H \times W \times C_M$ value matrices that the STM module produces. The second way the GC module improves efficiency is that it adds the extracted context matrix to the stored context matrix, thereby keeping constant memory usage however many frames are processed. In contrast, the STM module concatenates the obtained key and value matrices to the original key and value matrices in the memory, thus having a linear growth of memory with the number of frames.

For the computation on the current frame, i.e. the context distribution step, our GC only needs to perform a light weight matrix product of size $C_M \times C_N$ and $C_N \times HW$ with $C_M C_N HW$ multiplications involved. In contrast, the last step in the memory reading of STM module calculate a matrix product of size $HWT \times HW$ and $HW \times C_M$ ($C_M H^2 W^2 T$ multiplications), which has much larger memory usage and computation cost than GC and has linear complexities with respect to the time T . To get a more intuitive comparison of the two, we calculate the computation and resources needed in this step for the case where the input to the encoder is of size 384×384 , $C_M = 512$, and $C_N = 128$ (the default setting in STM). The detailed numbers are listed in Table 1. It is noticeable that our GC module has great advantages over STM in terms of both computation and memory cost, especially when the number of processed frames t becomes large along the processing.

3.2. Implementation

Our encoder and decoder design is the same as STM [22]. We use ResNet50 [10] as the backbone for both the memory encoder and query encoder where the memory encoder takes four-channel inputs and the query encoder takes three-channel inputs. The feature map at res4 is used to generate the key and value maps. After the context distribution operation, the feature is compressed to have 256 channels and fed into the decoder. The decoder takes this

Method	t	FLOPS	Memory
STM	0	0.2 G	4 MB
	10	2.1 G	40 MB
	100	21.2 G	394 MB
GC (ours)	any	0.04 G	1 MB

Table 1. The complexity comparison of the memory read operation in STM [22] and context distribution in our GC module. The memory usage is calculated using the float32 data type.

GC feature size	$\mathcal{J}\&\mathcal{F}$	# parameters	Runtime (s)
512×128	86.6	38 M	0.040
512×512	86.1	46 M	0.046

Table 2. Study on the size of global context feature ($C_M \times C_N$). This result is on DAVIS 2016 test set and the $\mathcal{J}\&\mathcal{F}$ is a segmentation accuracy metric (details in Sec. 4).

low-resolution input feature map and gradually upscales it by a scale factor of two each time. Skip connection is used to retrieve and fuse the feature map at the same resolution in query encoder with bilinearly upsampled feature map from the previous stage of the decoder. The key and value generation (i.e. k, q, v in Equation (1) and (3)) are implemented using 3×3 convolutions. In our implementation, we set $C_M = 512$ and $C_N = 128$. We have tested with larger feature sizes which introduce more complexities, but we do not observe accuracy gain in segmentation (see Table. 2).

3.3. Training

Our training process mainly contains two stages. We first pretrain the network using simulated videos generated from static images. After that we fine-tune this pretrained model on the video object segmentation datasets. We minimize the cross-entropy loss and train our model using the Adam [16] optimizer with a learning rate of 10^{-5} .

Pre-training on images. We follow the successful practice in [22, 30, 31] that pre-trains the network using simulated video clips with frames generated by applying random transformation to static images. We use the images from the MSRA10K [6], ECSSD [33], and HKU-IS [17] datasets for the saliency detection task. We found these datasets cover more object categories than those semantic segmentation or instance segmentation datasets [8, 9, 19]. This is more suitable for our purpose to build a general video object segmentation model. There are in total about 15000 images with object masks. A synthetic clip contains three frames are then generated using image transformations. We use random rotation $[-30^\circ, 30^\circ]$, scaling $[-0.75, 1.25]$, thin plate spline (TPS) warping (as in [23]), and random cropping for the video data simulation. We use 4 GPUs and set the batch

size to be 8. We run the training for 100 epochs, and it takes one day to finish the pre-training.

Fine-tuning on videos. After training on the synthetic video data, we fine-tune our pre-trained model on video object segmentation datasets [24, 25] at 480p resolution. The learning rate is set to 10^{-6} and we run this fine-tuning for 30 epochs. Each training sample contains several temporally ordered frames sampled from the training video. We use random rotation, scaling, and random frame sampling interval in $[1, 3]$ to gain more robustness to the appearance changes over a long time. We have tested different clip lengths (e.g. 3, 6, 9 frames) but did not observe performance gains on lengths greater than three. Therefore, we stick to three-frame clips. In the training, the network infers the object mask on the second frame and back propagates the error. Then, the soft mask from the network output is fed to the encoder to infer the mask on the third frame without thresholding as in [22].

4. Experimental Results

We evaluate our method and compare it with others on the DAVIS benchmarks [24, 25]. The object segmentation mask evaluation metrics used in our experiments are the average region similarity (\mathcal{J} mean), the average contour accuracy (\mathcal{F} mean), and the average of the two ($\mathcal{J}\&\mathcal{F}$ mean). The DAVIS benchmarks [24, 25] contain single-object and multiple-object segmentation tasks.

4.1. DAVIS 2016

DAVIS 2016 [24] is a widely used benchmark dataset for single-object segmentation in videos. It contains 50 videos among which 30 videos are for training and 20 are for testing. There are in total 3455 frames annotated with a single object mask for each frame.

We list the quantitative results for representative works on the DAVIS 2016 validation set in Table 3, including the most recent STM [22] and RANet [30]. To show their best performance, we directly quote the numbers posted on the benchmark website or in the papers. We can see that online-learning methods can get higher scores in most metrics. However, recent works of STM [22] and RANet [30] demonstrate comparable results without online learning. Note that STM [22] reported a higher score using additional datasets [32], which is not quoted here for a fair comparison. Overall, the scores for our GC are among the top, including getting the highest \mathcal{J} mean score. This is likely due to the hybrid loss used in our fine-tuning.

Furthermore, for a more intuitive comparison, we plot the runtime in terms of average FPS and accuracy in terms of $\mathcal{J}\&\mathcal{F}$ mean for different methods in Fig. 4. We test the speed on one Tesla P40. It can be seen that although the online-learning methods (e.g. [1, 20, 21]) can produce highly accurate results, their speeds are extremely slow due

Method	Time (s)	$\mathcal{J}\&\mathcal{F}$	\mathcal{J}	\mathcal{F}
OSVOS [2]	7	80.2	79.8	80.6
Lucid [15]	-	83.0	83.9	82.0
CINM [1]	>30	84.2	83.4	85.0
OnAVOS [28]	13	85.5	86.1	84.9
OSVOS-S [21]	4.5	86.6	85.6	87.5
PRemVOS [20]	>30	86.8	84.9	88.6
DyeNet [18]	2.32	-	86.2	-
SiamMask [29]	0.03	70.0	71.7	67.8
OSMN [35]	0.13	73.5	74.0	72.9
PML [3]	0.28	77.4	75.5	79.3
VidMatch [11]	0.32	-	81.0	-
FAVOS [4]	1.8	81.0	82.4	79.5
FEELVOS [27]	0.5	81.7	80.3	83.1
RGMP [31]	0.13	81.8	81.5	82.0
AGAME [14]	0.07	81.9	81.5	82.2
RANet [30]	0.13	85.5	85.5	85.4
STM* [22]	0.15	86.5	84.8	88.1
GC (ours)	0.04	86.6	87.6	85.7

Table 3. The quantitative comparison on the DAVIS 2016 validation set. The results are sorted for online and non-online methods respectively according to $\mathcal{J}\&\mathcal{F}$ mean. The highest scores in each category are highlighted in bold.

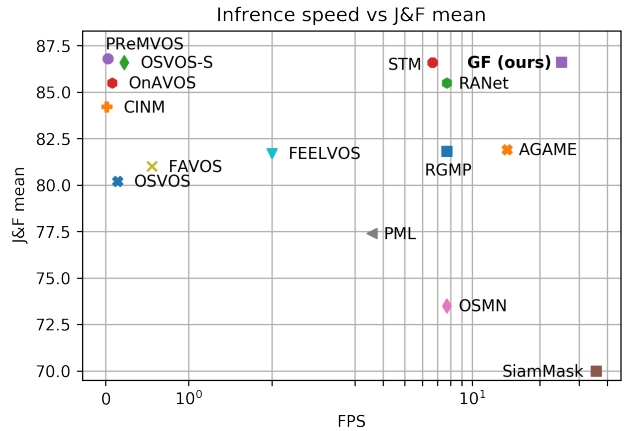


Figure 4. The speed (FPS) v.s. accuracy ($\mathcal{J}\&\mathcal{F}$ mean) comparison on the DAVIS 2016 validation set at 480p resolution.

to the time consuming online learning process. The methods without online learning (e.g. [3, 31, 35]) are fast but have lower accuracy. The most recent works STM [22] and RANet [30] can get segmentation accuracy comparable to online-learning method while maintaining faster speed (STM [22] 0.15 s, RANet [30] 0.12 s to process a 480p

frame¹). Our GC boosts the speed further (0.04 s) and still maintains high accuracy. Note that the videos in the DAVIS datasets are all short (<100 frames). If running on longer videos, our speed advantage over STM [22] will become more remarkable as STM has a linear time complexity with respect to the video length. While SiamMask [29] is the only method faster than our GC, its accuracy is very unsatisfactory compared to other methods. This demonstrates our GC is both fast and accurate which makes it a practical solution to the video object segmentation problem.

4.2. DAVIS 2017

DAVIS 2017 is an extension of DAVIS 2016 that contains video with multiple objects annotated per frame. It has 60 videos for training and 30 videos for testing. We do not use any additional module for multi-object segmentation which [22, 30] used, but simply treat each object individually. We still train the network to produce binary mask for the object. In testing, we use the network to get the soft probability map for each object separately and use a soft-max operation as post-processing on the maps for all objects in the frame to produce the multi-label segmentation mask.

Table 4 summarizes the performance of existing methods and compare them with ours on the DAVIS 2017 dataset. The multi-object scenarios is more challenging than the single object ones due to the interactions and occlusions among multiple objects. It can be seen that again online-learning methods e.g. [1, 20] get decent scores in all metrics, but have longer runtime. For non-online methods, STM [22] ranks the highest overall. Note that STM [22] reports a higher score using additional datasets [32], which is not quoted here for a fair comparison. Our model can get almost identical performance with STM [22] but runs faster.

4.3. Qualitative Results

Fig. 5 shows visual examples of our segmentation results on the DAVIS 2016 and DAVIS 2017 test datasets. As can be seen in the figure, our GC module can handle many challenging cases such as appearance changes (row 1), size changes (row 3, 5, and 6), and occlusions (row 2 and 4).

4.4. Visualization of the Global Context Module

Fig. 6 shows visualization of global context module. The first row shows the frame and the rest shows the visualizations of two channels of the corresponding global context keys from context extraction phase of the global context module. The brighter a pixel is, the larger the weight of the pixel in the weighted summation that produces the corresponding global feature vectors. It can be seen that the sec-

Method	$\mathcal{J}\&\mathcal{F}$	\mathcal{J} Mean	\mathcal{F} Mean
OSVOS [2]	60.3	56.6	63.9
OnAVOS [28]	65.4	61.6	69.1
OSVOS-S [21]	68.0	64.7	71.3
CINM [1]	70.6	67.2	74.0
PRemVOS [20]	77.8	73.9	81.8
OSMN [35]	54.8	52.5	57.1
SiamMask [29]	56.4	54.3	58.5
FAVOS [4]	58.2	54.6	61.8
VidMatch [11]	-	56.5	-
RANet [30]	65.7	63.2	68.2
RGMP [31]	66.7	64.8	68.6
FEELVOS [27]	69.1	65.9	72.3
AGAME [14]	70.0	67.2	72.7
STM* [22]	71.6	69.2	74.0
GC (ours)	71.4	69.3	73.5

Table 4. The quantitative comparison on DAVIS 2017 validation set. The upper parts are all online-learning methods. The results are sorted for online and non-online methods respectively according to $\mathcal{J}\&\mathcal{F}$ mean. The highest scores in each category are highlighted in bold.

ond row focuses on object centers, and the third row places most attention on the ground.

4.5. Limitations

Fig. 7 shows a limitation of our GC method. In multi-object segmentation, sometimes GC will erroneously transfer the mask of one object to another one in the same object category when the two overlap together, like the dog in red (row 1) and the gold fish in green (row 2).

5. Conclusion

We have presented a practical solution to the problem of semi-supervised video object segmentation. It is achieved by a novel global context module that effectively and efficiently captures the object segmentation information in all processed frames with a set of fixed-size features. The evaluation on benchmark datasets shows that our method gets top performance, especially on the single-object DAVIS 2016 dataset, and runs at a much faster speed than all top-performing methods, including the state-of-the-art STM. We believe that our GC network has the potential to become a core module in practical video object segmentation tools. In the future, we want to optimize it further to make it suitable for running on portable devices like tablets and mobile phones. Applying the global context module to other video-related computer vision problems is also of our interest.

¹RANet [30] reported a faster runtime in the paper using half-precision computation which is disabled in our test for fair comparison

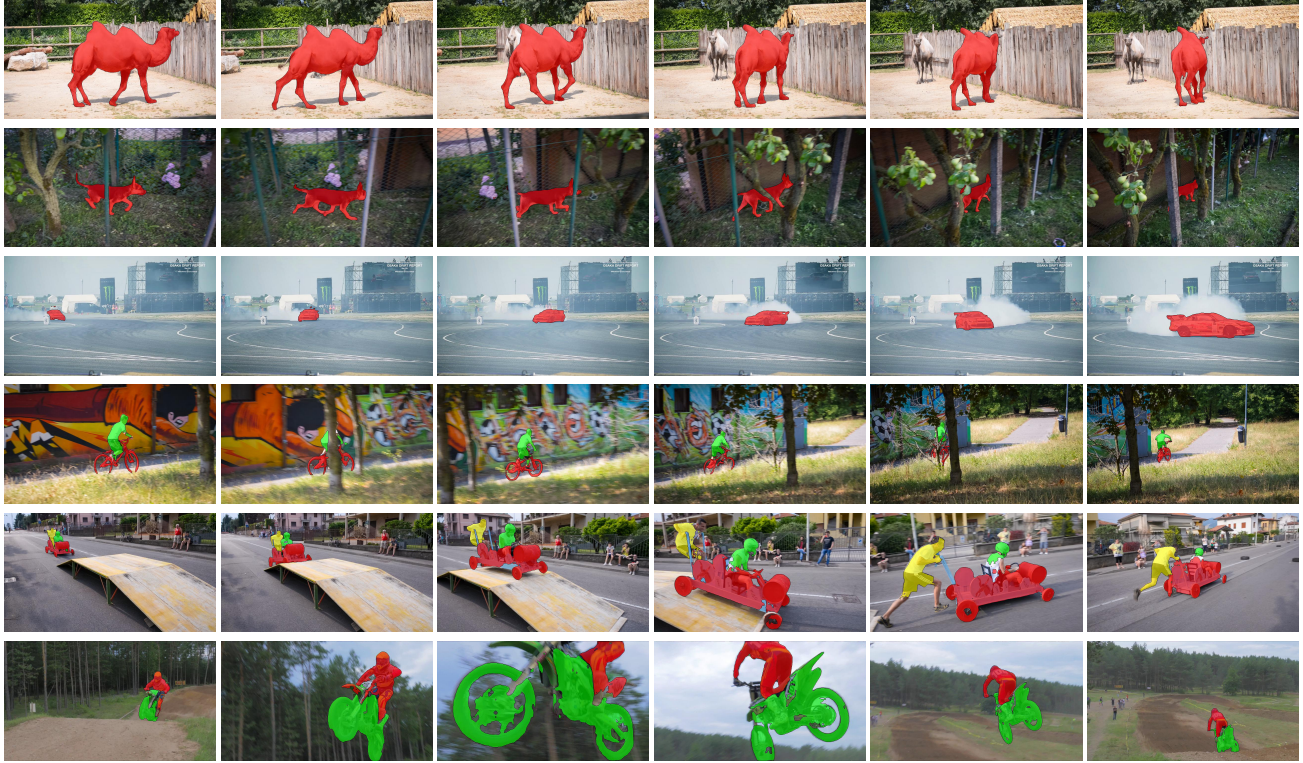


Figure 5. The visual results of our GC on DAVIS dataset.



Figure 6. Visualization of global context keys.

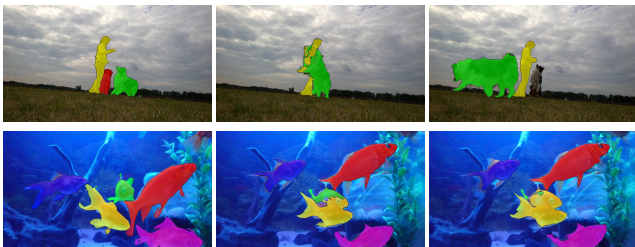


Figure 7. Two cases our GC model fails.

References

- [1] Linchao Bao, Baoyuan Wu, and Wei Liu. Cnn in mrf: Video object segmentation via inference in a cnn-based higher-order spatio-temporal mrf. In *CVPR*, 2018. 2, 6, 7
- [2] Sergi Caelles, Kevis-Kokitsi Maninis, Jordi Pont-Tuset, Laura Leal-Taixé, Daniel Cremers, and Luc Van Gool. One-shot video object segmentation. In *CVPR*, 2017. 1, 2, 6, 7
- [3] Yuhua Chen, Jordi Pont-Tuset, Alberto Montes, and Luc Van Gool. Blazingly fast video object segmentation with

- pixel-wise metric learning. In *CVPR*, 2018. 2, 6
- [4] Jingchun Cheng, Yi-Hsuan Tsai, Wei-Chih Hung, Shengjin Wang, and Ming-Hsuan Yang. Fast and accurate online video object segmentation via tracking parts. In *CVPR*, 2018. 1, 6, 7
- [5] Jingchun Cheng, Yi-Hsuan Tsai, Shengjin Wang, and Ming-Hsuan Yang. Segflow: Joint learning for video object segmentation and optical flow. In *ICCV*, 2017. 2
- [6] Ming-Ming Cheng, Niloy J Mitra, Xiaolei Huang, Philip HS Torr, and Shi-Min Hu. Global contrast based salient region detection. *TPAMI*, 37(3):569–582, 2014. 5
- [7] Alexey Dosovitskiy, Philipp Fischer, Eddy Ilg, Philip Hausser, Caner Hazirbas, Vladimir Golkov, Patrick Van Der Smagt, Daniel Cremers, and Thomas Brox. FlowNet: Learning optical flow with convolutional networks. In *ICCV*, 2015. 2
- [8] M. Everingham, L. Van Gool, C. K. I. Williams, J. Winn, and A. Zisserman. The pascal visual object classes (voc) challenge. *International Journal of Computer Vision*, 88(2):303–338, June 2010. 5
- [9] Bharath Hariharan, Pablo Arbelaez, Lubomir Bourdev, Subhransu Maji, and Jitendra Malik. Semantic contours from inverse detectors. In *International Conference on Computer Vision (ICCV)*, 2011. 5
- [10] Kaiming He, Xiangyu Zhang, Shaoqing Ren, and Jian Sun. Deep residual learning for image recognition. In *CVPR*, 2016. 5
- [11] Yuan-Ting Hu, Jia-Bin Huang, and Alexander G Schwing. Videomatch: Matching based video object segmentation. In *ECCV*, 2018. 2, 6, 7
- [12] Eddy Ilg, Nikolaus Mayer, Tonmoy Saikia, Margret Keuper, Alexey Dosovitskiy, and Thomas Brox. FlowNet 2.0: Evolution of optical flow estimation with deep networks. In *CVPR*, 2017. 2
- [13] Won-Dong Jang and Chang-Su Kim. Online video object segmentation via convolutional trident network. In *CVPR*, 2017. 2
- [14] Joakim Johnander, Martin Danelljan, Emil Brissman, Fahad Shahbaz Khan, and Michael Felsberg. A generative appearance model for end-to-end video object segmentation. In *CVPR*, 2019. 6, 7
- [15] Anna Khoreva, Rodrigo Benenson, Eddy Ilg, Thomas Brox, and Bernt Schiele. Lucid data dreaming for video object segmentation. *IJCV*, 127(9):1175–1197, 2019. 2, 6
- [16] Diederik P Kingma and Jimmy Ba. Adam: A method for stochastic optimization. In *ICLR*, 2014. 5
- [17] Guanbin Li and Yizhou Yu. Visual saliency based on multi-scale deep features. In *CVPR*, 2015. 5
- [18] Xiaoxiao Li and Chen Change Loy. Video object segmentation with joint re-identification and attention-aware mask propagation. In *ECCV*, 2018. 2, 6
- [19] Tsung-Yi Lin, Michael Maire, Serge Belongie, James Hays, Pietro Perona, Deva Ramanan, Piotr Dollár, and C Lawrence Zitnick. Microsoft coco: Common objects in context. In *European conference on computer vision*, pages 740–755. Springer, 2014. 5
- [20] Jonathon Luiten, Paul Voigtlaender, and Bastian Leibe. Premvos: Proposal-generation, refinement and merging for video object segmentation. In *ACCV*, 2018. 2, 6, 7
- [21] K-K Maninis, Sergi Caelles, Yuhua Chen, Jordi Pont-Tuset, Laura Leal-Taixé, Daniel Cremers, and Luc Van Gool. Video object segmentation without temporal information. *TPAMI*, 41(6):1515–1530, 2018. 1, 2, 6, 7
- [22] Seoung Wug Oh, Joon-Young Lee, Ning Xu, and Seon Joo Kim. Video object segmentation using space-time memory networks. In *ICCV*, 2019. 2, 3, 4, 5, 6, 7
- [23] Federico Perazzi, Anna Khoreva, Rodrigo Benenson, Bernt Schiele, and Alexander Sorkine-Hornung. Learning video object segmentation from static images. In *CVPR*, 2017. 1, 2, 5
- [24] Federico Perazzi, Jordi Pont-Tuset, Brian McWilliams, Luc Van Gool, Markus Gross, and Alexander Sorkine-Hornung. A benchmark dataset and evaluation methodology for video object segmentation. In *CVPR*, 2016. 6
- [25] Jordi Pont-Tuset, Federico Perazzi, Sergi Caelles, Pablo Arbeláez, Alexander Sorkine-Hornung, and Luc Van Gool. The 2017 davis challenge on video object segmentation. *arXiv:1704.00675*, 2017. 6
- [26] Jae Shin Yoon, Francois Rameau, Junsik Kim, Seokju Lee, Seunghak Shin, and In So Kweon. Pixel-level matching for video object segmentation using convolutional neural networks. In *ICCV*, 2017. 2
- [27] Paul Voigtlaender, Yuning Chai, Florian Schroff, Hartwig Adam, Bastian Leibe, and Liang-Chieh Chen. Feelvos: Fast end-to-end embedding learning for video object segmentation. In *CVPR*, 2019. 1, 2, 6, 7
- [28] Paul Voigtlaender and Bastian Leibe. Online adaptation of convolutional neural networks for video object segmentation. In *BMVC*, 2017. 1, 2, 6, 7
- [29] Qiang Wang, Li Zhang, Luca Bertinetto, Weiming Hu, and Philip HS Torr. Fast online object tracking and segmentation: A unifying approach. In *CVPR*, 2019. 6, 7
- [30] Ziqin Wang, Jun Xu, Li Liu, Fan Zhu, and Ling Shao. Ranet: Ranking attention network for fast video object segmentation. In *ICCV*, 2019. 1, 2, 5, 6, 7
- [31] Seoung Wug Oh, Joon-Young Lee, Kalyan Sunkavalli, and Seon Joo Kim. Fast video object segmentation by reference-guided mask propagation. In *CVPR*, 2018. 1, 2, 5, 6, 7
- [32] Ning Xu, Linjie Yang, Yuchen Fan, Jianchao Yang, Dingcheng Yue, Yuchen Liang, Brian Price, Scott Cohen, and Thomas Huang. Youtube-vos: Sequence-to-sequence video object segmentation. In *ECCV*, 2018. 6, 7
- [33] Qiong Yan, Li Xu, Jianping Shi, and Jiaya Jia. Hierarchical saliency detection. In *CVPR*, 2013. 5
- [34] Linjie Yang, Yanran Wang, Xuehan Xiong, Jianchao Yang, and Aggelos K Katsaggelos. Efficient video object segmentation via network modulation. In *CVPR*, 2018. 1
- [35] Linjie Yang, Yanran Wang, Xuehan Xiong, Jianchao Yang, and Aggelos K Katsaggelos. Efficient video object segmentation via network modulation. In *CVPR*, 2018. 2, 6, 7